Modelling Simul. Mater. Sci. Eng. **8** (2000) 649–664. Printed in the UK PII: S0965-0393(00)14743-6

Wavelet methods for analysing and bridging simulations at complementary scales—the compound wavelet matrix and application to microstructure evolution

G Frantziskonis† and P A Deymier‡

† Department of Civil Engineering and Engineering Mechanics, University of Arizona, Tucson, AZ 85721, USA

‡ Department of Materials Science and Engineering, University of Arizona, Tucson, AZ 85721, USA

Received 20 January 2000, accepted for publication 8 June 2000

Abstract. We introduce a novel wavelet-based compound matrix to bridge models (Lennard-Jones model simulated with molecular dynamics and a lattice Q-states Potts model with a Monte Carlo simulation) that describe grain growth over different ranges of spatial and time scales. The compound wavelet matrix provides full statistical information on the microstructure at the range of scales that is the union of those handled by the two models.

1. Introduction

The polycrystalline state of matter is multilevel with information at several scales. Point defects, dislocations, grain boundaries, grain boundary junctions and iso-orientation aggregates of grains span a very wide range of scales from the atomic to the mesoscopic to the macroscopic. The geometric complexity is complicated further by the interactions among structural features at different scales. To cite only a few: grain boundaries, which may act as a source or sink for point defects; grain boundary/dislocation (from bulk to primary to secondary grain boundary dislocations) interactions and their effect on grain boundary migration; grain boundary/grain boundary interactions during grain annihilation or topological transitions such as grain switching; and low-energy/high-energy grain boundary interaction in anisotropic polycrystals.

In addition to the structural hierarchy of polycrystalline materials it is essential to also recognize their dynamical nature [1]. Processes at various length scales usually possess different relaxation times, suggesting that in addition to the spatial hierarchy a temporal one also exists. For instance, although point defects may exist at equilibrium, dislocations and grain boundaries may never be at equilibrium. Microstructures are therefore only a reflection of the fact that a polycrystalline material has not had enough time to reach equilibrium (with the lowest energy in the single crystal state). Also, microstructures are path and history dependent, adding further complexity in understanding and controlling their evolution.

Normal grain growth achieves a quasi-stationary distribution of grain sizes after a transient period. Understanding grain growth necessitates an accurate description of the spatial and temporal evolution of polycrystals during this transient and, more importantly, the quasi-stationary stage of the process. We discuss the latter more and review some studies that stress the importance of spatial correlations and scales.

0965-0393/00/050649+16$30.00

Repeated experimental observations in a wide variety of materials have shown that normal grain growth is characterized by a microstructural homogeneity and a scaling property [2]. Microstructural homogeneity is associated with a narrow distribution of grain sizes and a maximum grain size of the order of 2.5 to 3 times the arithmetic mean grain size. This has been found to persist as growth proceeds, resulting in a time invariance of the grain size distribution when normalized to the mean grain size. Normal grain growth is therefore generally described within the context of a time scaling regime in which the normalized grain size distribution does not change with time. Within this scaling regime, grain coarsening proceeds with only a change in length scale, often characterized by the grain radius $\langle R \rangle$. The kinetics of normal grain growth in two dimensions is often characterized by a law of the form $\langle R \rangle = Kt^{1/2}$ where K is constant and t is time. Established theories for grain growth [3, 4] assume that all grain boundaries have the same energy leading to shrinkage of those grains with less than six sides and growth of those with more than six sides. Since the radius of curvature is directly proportional to the grain diameter, the mean grain size increases as the square root of time.

Processes involving evolution of a microstructure have been studied extensively, primarily in a statistical fashion. Normal grain growth in polycrystalline materials is driven by a reduction in excess interfacial energy, and this reduction takes place by elimination of grains. Mean field approaches have phenomenologically related the time evolution of the average grain size to an interfacial driving force. Such a relation may be used to form the continuity equation for the distribution of grain sizes, the solution of which provides a statistical description of microstructure evolution. Correlation effects (e.g. a characteristic spatial arrangement of the grains occurs in correspondence to their relative sizes) have been shown to give better agreement between experimental and calculated size distributions [5–8]. Furthermore, stochastic theories of grain growth are being used for treating grain growth as a geometrically complex process [9–11]. In these works, grain growth possesses a deterministic drift component and a stochastic component. Grain growth is then described by a Fokker–Planck continuity equation dealing with the grain size distribution and its evolution in time. The drift component arises from the curvature effect (i.e. the driving force in the mean field models) that causes small grains to shrink and large ones to grow. The stochastic nature of the process has been interpreted on the basis of local statistical variations of how individual grains evolve differently depending on the geometrical characteristics of the surrounding grains.

The effect of grain boundary anisotropy on growth kinetics has been examined within the context of stochastic theories of grain growth [12]. There are theoretical and experimental indications that anisotropic microstructures contain clusters composed of grains belonging to low-angle or special categories [13–16]. It is anticipated that low-energy grain boundaries evolve at rates smaller than those of high-energy boundaries. Clusters of grains separated by low-energy grain boundaries may survive until some neighbouring grain with a different crystallographic orientation grows to that size and starts interacting with that cluster. To account for the spatial variability of grain boundary energies, the microstructure possesses a new state variable that scales as the cluster size. This cluster length scale, larger than the mean grain size, is at the origin of the slower kinetics. The survival of clusters of small grains with similar grain boundary energies leads to a broader grain-size distribution.

In spite of the numerous studies of normal grain growth, a complete picture of grain growth of polycrystalline materials is still to be achieved, the main reason being that the overall kinetics are controlled by geometrical features and relaxation times at largely different scales. In particular, grain growth kinetics with anisotropic grain boundaries is governed by physics at three different scales, namely the atomic scale at the level of individual grain boundaries, a larger scale associated with the grain size and the even larger scale of clusters of grains with similar grain boundary energy. It would be desirable to simulate the outstanding problem of

two-dimensional (2D) anisotropic grain growth within the framework of an atomistic computer simulation technique (such as molecular dynamics (MD)) that can capture the physics of the phenomenon from the atomic scale and up. However, to study grain growth at the scale associated with clusters of grains as well as its interplay with processes at the two other smaller scales, one would need to simulate an excessively large number of atoms for an excessively long time, unachievable with present and foreseeable computer capabilities.

Several 'mesoscopic' computational techniques have been developed to simulate the evolution of the microstructure in polycrystalline materials. Some of these include Monte Carlo (MC) simulation of lattice models, such as the Q-states Potts model [17], Continuous models [18] and the vertex model [19]. Each of these techniques is usually limited to treating grain growth at specific scales by either the physics involved or by computer power. For instance, 'mesoscopic' simulation techniques based on lattice models do not include atomic scale features (such as in atomistic models) since grain orientations are often represented by a spin state. In materials, given the hierarchy of spatial scales in their microstructures and the hierarchy of time scales during their evolution [1], it is important to couple simulation techniques such as MD and mesoscopic models to study grain growth over the complete spectrum of scales.

Most of the modern simulation methods for coupling length scales can be characterized as either serial or concurrent. In serial methods a set of calculations at a fundamental level (small length scale) is used to evaluate parameters for use in a more phenomenological model to describe the phenomenon of interest at a longer length scale. For example, atomistic simulations can be used to feed the constitutive behaviour of finite elements, which are then used to simulate a larger-scale problem [20]. Typically, the constitutive behaviour of each element results from an infinitely large MD simulation that is realized by using periodic boundary conditions for a small region. Concurrent methods rely on different computational methodologies applied to different regions of a material. For example, the problem of crack propagation is a problem that was tackled early on (and still is) by atomic simulations techniques near the tip of a crack where large deformations (even bond breakage) occur and a continuum approaches at large distances from the tip of the crack. This has been addressed by dividing space into two regions: namely the tip of the crack where the material is treated atomistically with MD and the rest of the material modelled as a continuum via the finite-element method [21, 22]. One of the main difficulties of this method is that the time evolution of the process is controlled by the region with the slowest dynamics (MD, for example). Another difficulty resides in the establishment of a seamless interface between the two regions.

In this paper, we design and present the footing for a novel multiscale approach based on wavelets that can establish a bridge between simulation techniques, capturing the physics of grain growth at significantly different scales as long as there exists a region of overlap in the domain of scales. The compound wavelet matrix (CWM) method introduced herein, in which two computational methodologies (MD simulation of the Lennard-Jones (L-J) system and MC simulation of the Q-states Potts model) are applied to a region of material simultaneously at the coarse and the fine spatial scales, is different from the other methods used for coupling length scales. Matrices of the wavelet coefficient are produced from energy maps representing the spatial distribution of the local excess energy in the microstructures obtained with both methodologies. The full description of the material is then obtained by merging the matrices of the wavelet coefficients representing the material at different scales through the CWM method. The CWM then characterizes the materials over a range of scales that is the union of the scales treated by the two methodologies. This method possesses several advantages compared to existing methods. First, it does not assume *a priori* that a collection of small microscale systems is equivalent to a microscale-based model of a large system. Second, the

simulation time of the coarsest methodology is not controlled by the methodology with the slowest dynamics.

In order to present an illustrative example of the CWM method applied to two-dimensional grain growth, we consider an MD simulation of a (2D) L-J system and a MC simulation of a Q-states Potts model that can overlap over a range of spatial and time scales. We illustrate how wavelet transformation is employed to analyse the microstructures obtained from the two simulation methods and to identify the scale of spatial correlations and their time evolution during the growth process. Then, we illustrate the feasibility of bridging these simulations. This is accomplished by demonstrating the overlap in scale of the 'mesoscopic' Q-states Potts model with the atomistic L-J model and constructing the CWM. We consider bridging these two models mainly in the spatial domain. However, the wavelet approach is general enough to extend beyond these two (atomistic and mesoscopic) scales, for example by employing and bridging a finite-element technique at coarser scales and, also, incorporating temporal scaling.

The paper is organized as follows. In section 2 we review briefly the methods (MD and MC) as well as the models (L-J and Q-states Potts models). In this same section we also introduce the method of wavelet transformation for characterization of microstructures and the CWM method. Section 3 contains the results of the simulations as well as their analysis using wavelet transforms. We also give a demonstration of the CWM method applied to the phenomenon of grain growth. In section 4 we summarize the principal results of this study and draw some conclusions concerning the applicability of the CWM method.

2. Models and methods

2.1. Simulation methods

We consider simple and classical 'versions' of the two simulation methods (MD and MC) and concentrate on their bridging and their overlapping over a region of scales. The method of classical MD consists of solving simultaneously the equations of motions of an assembly of particles interacting with each other through some interatomic potential [23]. The MD method is atomistic and allows investigation of grain growth from the atomic scale up, yet it is limited (by computer power) to small numbers of particles (nowadays in the hundreds of millions) and short periods of time. We focus our investigation on generic 2D 6-12 L-J systems [23] with parameters $\varepsilon = 119.79$ K and $\sigma = 3.405$ Å. We first simulate a 2D L-J system containing 90 000 particles in a cell with an edge length of about 0.106 μm. Interactions between atoms are extended up to third nearest neighbours. A polycrystalline microstructure with fine grains is initially obtained by quenching a liquid. This initial microstructure is then evolved with a constant temperature–constant volume MD algorithm. The temperature is maintained at approximately 70% of the melting point. Periodic boundary conditions are used for about 400 000 MD integration time steps or nearly 1.7×10^{-9} s. After that time the total energy of the system has dropped by nearly 63%, thus a coarser microstructure is obtained. This microstructure is then characterized by calculating the excess atomic potential energy of each individual atom (relative to the potential energy of an atom in a perfect lattice at the same temperature). The excess atomic energy is then normalized by the total excess energy of the microstructure at $t = 0$. The spatial distribution of the normalized excess atomic energy is then mapped onto a 512×512 square matrix to obtain what will be referred to in the rest of the paper as an energy map. We note that the L-J system includes grain boundary anisotropy; that is, the grain boundary energy may vary depending upon the degree of misorientation between adjacent grains. A microstructure may therefore contain low-energy low-angle grain boundaries and high-energy high-angle grain boundaries. Moreover, the anisotropy in the

grain boundary energy also results at fixed misorientation from the inclination of the grain boundary plane.

In a MC simulation of grain growth with a Potts model, both spatial and 'MC time' scales are coarser than those in MD. The Potts model maps the microstructure onto a discrete lattice that is coarser than the atomic scale, and the 'spin' state $S = 1, \ldots, Q$ of each lattice site represents the orientation of the grain in which it is embedded [17]. A grain boundary exists between two adjacent lattice sites with different orientations. We employ a Potts model with a square lattice containing 128×128 sites and $Q = 10$ (see following discussion) with only nearest-neighbour interactions. This model is designed to represent a piece of material with dimensions similar to those of the MD system. Periodic boundary conditions are applied onto the Potts model. We have chosen a square lattice to mimic anisotropic grain growth. Since the L-J microstructure includes grain boundary anisotropy we wish to include some level of anisotropy in the Potts model. For the sake of simplicity, the Potts model we use here does not include orientational anisotropy; the energy associated with two neighbouring sites with different spin orientations does not vary with the magnitude of the difference in spin. The Potts model, however, incorporates some degree of anisotropy associated with the grain boundary inclination since a grain boundary running parallel to the principal directions of the square lattice does not possess the same energy per unit length as a grain boundary that runs along the diagonal to the lattice. In that case, the grain boundary energy may vary by a factor of up to $\sqrt{2}$ given a higher degree of grain boundary anisotropy than could be achieved with a triangular lattice. Furthermore, it was shown that finite temperature simulations of Potts models with the square lattice and first-nearest-neighbour interaction produced microstructures with topological moments comparable to those measured for 2D grain growth of real metals [24].

A MC algorithm is used to evolve this model. The thermal energy, kT (where T is the temperature and k is Boltzmann's constant) is $0.2J$ with J being the energy associated with two misoriented neighbouring sites. This temperature is sufficient to alleviate the pathological problem of growth on first-nearest-neighbour square lattices at low temperature. Indeed it is known that for the square lattice with nearest-neighbour interaction, domain grain growth at zero temperature stops when the domain vertices absorb all initial wall curvature [24]. However, Anderson *et al* [25] have shown that at finite temperature the square lattice with nearest-neighbour interaction and $Q > 3$ exhibits significant coarsening, grain boundary curvature and a microstructure resembling that obtained with a triangular lattice. Under the goal of this work to demonstrate the bridging of the two simulations in their simple form, we have used $Q = 10$, on a square lattice. Improvements on each of the two simulation methods should increase the effectiveness of the CWM. This is addressed further in the following paragraphs.

Initial microstructures are produced from totally random configurations after 4×10^6 MC moves. A total of four such initial configurations corresponding to microstructures optically similar to the initial configuration of the L-J system are thus obtained (the similarity between the initial Potts microstructures and the initial L-J system was further confirmed by their wavelet transformation showing similar statistics at the equivalent scales). Subsequently, we run long MC simulations to anneal the initial microstructures, until the total energy averaged over the four systems decreased to nearly 63% of the average energy of the initial configurations. Matrices of size 128×128 containing the value of energy at every lattice site characterize the final MC microstructures. Note that the energy in the Potts model represents an excess energy relative to a perfectly ordered system (perfect crystal). Normalization of the energy at each lattice site by the total excess energy of the initial microstructure allows a direct comparison with the energy maps produced from the MD simulations.

In order to bridge the two simulation techniques, correspondence should be established between the MD and MC times and energies. Several approaches have been proposed in the

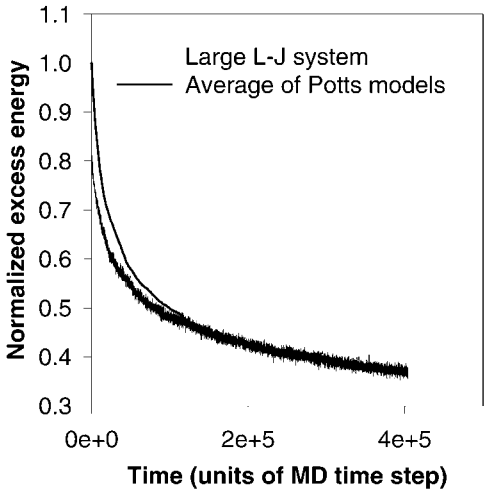

Figure 1. Excess energy against time obtained with the MD simulation of an L-J system (90 000 particles) and average of MC simulations of four Potts models with different initial configurations. The excess energy relative to the perfect crystal at the same temperature is normalized to the excess energy of the initial microstructure. The MC time is scaled to match the MD time (see text for details).

literature; for example MC time can be linearly related to real time [26]. The conversion from the MC time to real time has an implicit activation energy factor that corresponds to a jump. On the other hand, in the Potts model a grain boundary exists between two adjacent lattice sites with different orientations. Therefore, the time for reorientation of a lattice site may be related to the time for migration of a segment of a grain boundary. On this premise, a time conversion scheme, based on grain boundary migration, may be applicable [27]. Here, we establish a correspondence between the MD time step and the MC step by renormalizing the time it takes for the energy (normalized to the energy of the initial state) of the L-J system and of the Potts models to decrease to the same value. Figure 1 shows the time evolution of the total potential energy of the L-J system as well as the energy of the Q-states Potts models averaged over four MC simulations. Note that at early time the MD system and the Potts model do not agree; this may be due to the different physics in the early stages of relaxation, and this deserves further investigation. Yet, after this transient period, at later time, all simulations evolve similarly. The normalized energy maps corresponding to the initial and annealed microstructures of the L-J system as well as one of the Potts models are shown in figure 2. As illustrated in figures 1 and 2, the normalization of energy, energy maps and time allow the L-J system and Potts model to overlap.

2.2. Wavelet transform and the CWM method

Having established a correspondence between the L-J model and the Q-states Potts model of microstructures and their evolution, we now illustrate how wavelet transforms can be used to analyse microstructures scale-wise as well as bridge the L-J system to the Potts model.

2.2.1. Wavelet transform. A general goal of wavelet analysis is to describe graphs (signals, images) as the superposition of elementary functions [28]. There are several publications on this rather new subject; a large number of monographs with diverse applications can be found

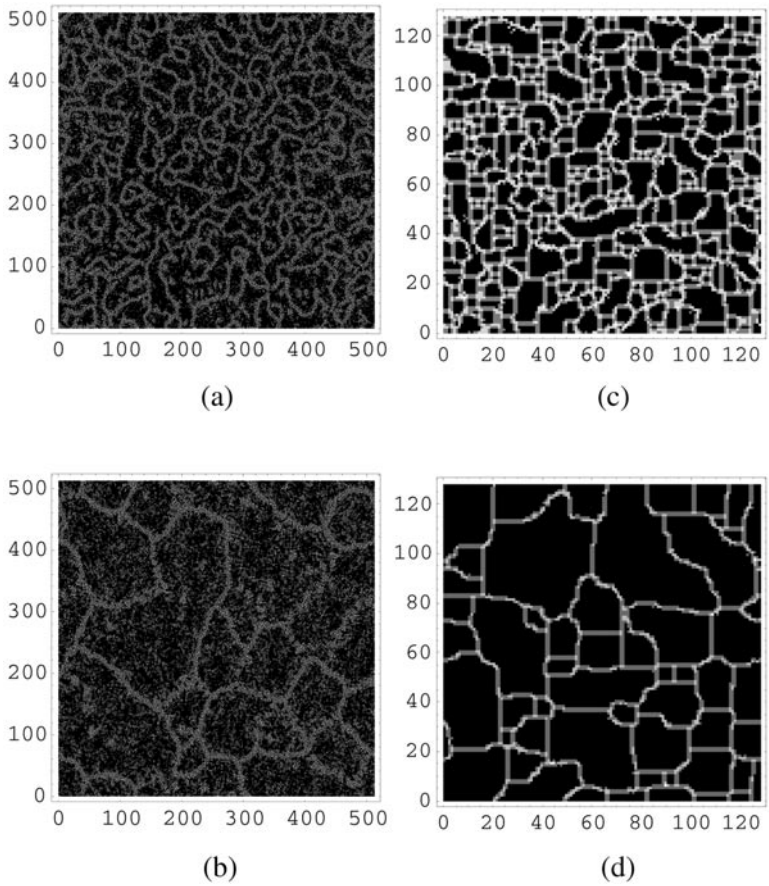

Figure 2. Grey-scale representation of the energy maps (see text for definition) for: (a) initial L-J system, (b) annealed L-J system, (c) one of the initial Potts models and (d) annealed Potts system. The energy increases from black to white.

in the literature. Wavelet transforms provide both scale and location (and/or time) information about a given function. In one dimension (easily extendable to higher dimensions) a wavelet $\psi(x)$ transforms a function $f(x)$ according to

$$W_f(a,b) = \int_{-\infty}^{\infty} f(x)\psi_{a,b}(x)\,\mathrm{d}(x). \tag{1}$$

The two-parameter family of functions, $\psi_{a,b}(x) = (1/\sqrt{a})\psi[(x-b)/a]$ is obtained from a single function, ψ, called the mother wavelet, through dilatations by the factor a^{-1} and translations by the factor b. The factor $1/\sqrt{a}$ is included for normalization purposes and, with it, all the wavelets have the same energy (other normalizations are also possible and often used in the literature). The scale parameter a can take any value on the positive real axis. The scalars defined in the above equation measure the fluctuations of $f(x)$ around point b, at the scale a. A wavelet analysis can either be continuous or discrete; the latter, based on orthogonal decomposition of a signal, can be performed with fast algorithms.

Given the wavelet coefficients $W_f(a,b)$ associated with a function f, it is possible to reconstruct f and/or construct its representation at a range of scales between s_1 and s_2 ($s_1 \leqslant s_2$)

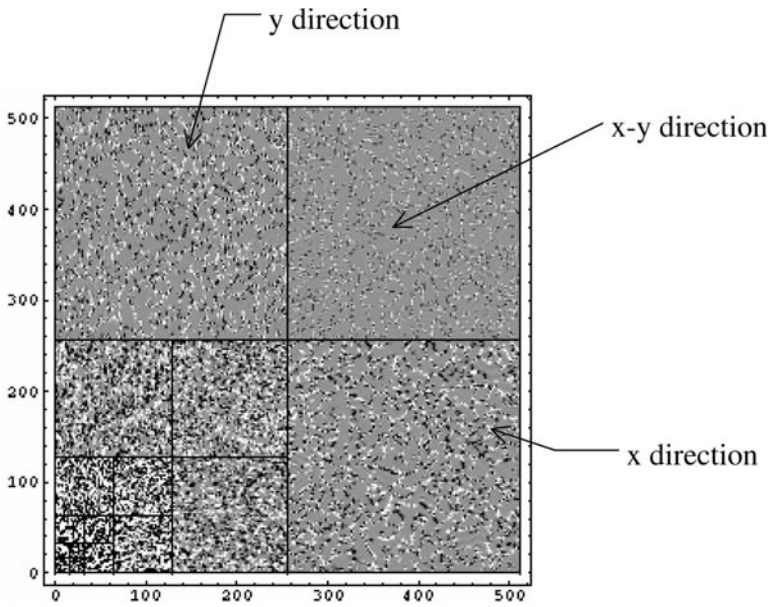

Figure 3. Grey-scale representation of the wavelet transform of the energy map shown in figure 2(a). All the decomposition matrices have been arranged in a (512 × 512) matrix. Details of the arrangement are shown for the finest decomposition 256 × 256. The magnitude of the wavelet coefficients increases from black to white.

through the inversion formula

$$f_{s_1,s_2}(x) = \frac{1}{c_\psi} \int_{s_1}^{s_2} \int_{-\infty}^{\infty} W_f(a,b)\psi_{a,b}(x)\,\mathrm{d}b\frac{\mathrm{d}a}{a^2} \tag{2}$$

where c_ψ is a constant. By setting $s_1 \to 0$, $s_2 \to \infty$, f is reconstructed. A 2D wavelet transform, in general, includes a transform in the x direction, a transform in the y direction and one in the x–y direction. For example, given an image of 512 × 512 pixels, the wavelet transform consists of three 256 × 256 matrices (one in the x direction, one in the y, and one in the x–y direction), three 128 × 128, and so on; each decomposition level is at half the resolution from the previous one. The final level of decomposition represents the image at the coarsest resolution. The construction of the matrix of the wavelet coefficients from an energy map is illustrated in figure 3.

We now perform the wavelet transform of the annealed microstructures (energy maps) obtained at the end of the MD simulation and of the four MC simulations. For all the wavelet related data presented in the sequence, we used biorthogonal symmetric wavelets with four vanishing moments and the corresponding so-called scaling functions [28]. A non-systematic study revealed that the use of other wavelets does not influence the results. Periodic boundary conditions were used for the wavelet transform, since both MC and MD data consider such boundary conditions.

As seen before, an energy map covers a range of scales. Here, we analyse the contribution of each scale to the energy of the microstructure. The energy associated with a given scale is evaluated from the wavelet representation of the energy maps at that same scale. For the wavelet representation of the energy map at scale n, the wavelet coefficients at all scales except those at n are set equal to zero; with this set of coefficients, the inverse wavelet transform is performed (see equation (2)). This inverse wavelet transform represents the spatial distribution

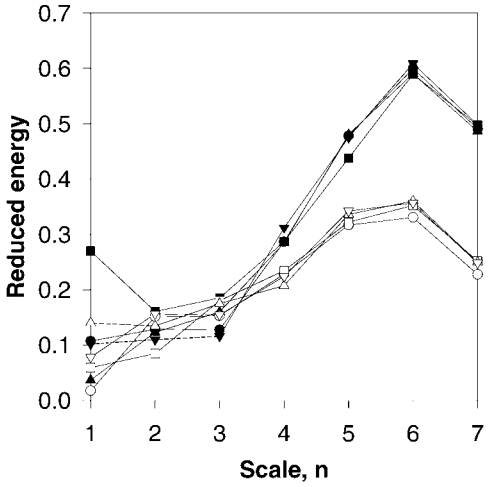

Figure 4. Energy of the wavelet representation of the energy maps of the Potts systems at specific scales. The horizontal axis or scale is defined as follows: scale 1 corresponds to 1×1 points in the wavelet matrix decomposition; scale 2 to 2×2 points; scale 3 to 4×4; ...; scale 7 to 64×64 points. The closed symbols are for the initial microstructures. The open symbols refer to the final microstructure annealed with the MC method.

of the contribution of scale n to the energy map. The total energy associated with scale n is then calculated as the sum of the energies in the representation at scale n. The energy map for the Potts model is reported on a 128×128 matrix. There are, therefore, seven scales for the Potts system at details of 64×64 points (represented by scale $n = 7$), 32×32 (scale $n = 6$) and, ..., 1×1 (scale $n = 1$) points. For the L-J system, the energy is mapped on a (512×512) matrix and contains nine scales corresponding to resolutions of 1×1 (scale $n = 1$), ..., 64×64 ($n = 7$), 128×128 ($n = 8$) and 256×256 ($n = 9$). The two systems overlap in the range of scale $n = 1$–7 with the L-J system giving supplemental information at the very fine scales of $n = 8$ and 9.

We report in figure 4 the energy as a function of scale calculated from the four initial and final Potts models. Overall the four systems behave in a similar manner. The initial microstructures exhibit a peak in energy at scale 6 (32×32 points), indicating that a significant amount of the energy of the microstructure in contained in microstructural features with a length scale of $1/32$ times the physical dimension of the system. This length corresponds effectively to the mean grain radius. The energy drops steadily as the scale decreases from six to one. This drop signifies the transition to a 'continuum' where the contribution to the energy from microstructural features such as grain boundaries is averaged out. In figure 4, a comparison between the energy against the scale of the initial and final microstructures can be used to shed light on the growth process. Indeed, the final Potts systems show a broader peak extending between scale 5 (16×16 points) and scale 6. This broadening is indicative of an increase in the mean grain size. Again at very coarse scales (small n), when approaching the continuum limit, the difference between the initial and final microstructures disappears. Note that due to the small number of points contributing to the energy at small scales (e.g. 1×1 for $n = 1$, 2×2 at $n = 2$, etc), the scattering in the data becomes larger as n decreases.

We illustrate further how wavelets can be used to analyse scales in microstructures, by considering the energy versus scale in the case of the final L-J system. Contrary to the MC simulation, the MD simulation is a dynamical technique. The energy maps such

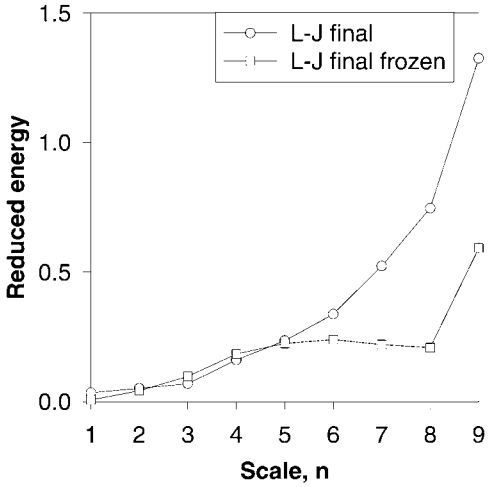

Figure 5. Energy of the wavelet representation of the energy maps of the final L-J system as a function of scale. The open circles represent the annealed microstructure (high temperature). The open squares are for the annealed microstructure subsequently frozen to remove thermal effects. The scales 1–7 are defined as in figure 4; scale 8 corresponds to 128 × 128 points and scale 9 to 256 × 256 points.

as those reported in figure 2 are constructed directly during the MD simulation. These energy maps therefore contain not only structural information (due to the defects), but also thermal information resulting from atomic vibrations. In figure 5 we present the two energy against scale plots for the final L-J system. The first is representative of the high-temperature microstructure. To produce the second we rapidly cooled, and maintained at a finite but very low temperature (∼0 K), the final L-J microstructure in order to reduce thermal agitation. The two plots are nearly indistinguishable for scales less than five since at these scales microstructural features and thermal agitation are smoothed out. The low-temperature microstructure freed from atomic vibration possesses a hump between scales 5 and 6. This hump is reminiscent of the maximum observed in the case of the final Potts systems and is again characteristic of an increasing mean grain size during the growth process. The sharp increase in the energy from scale 8 to scale 9 (256 × 256 points) can be associated with very fine structural features with a length scale of $1/256$ times the dimension of the system. This length corresponds to interatomic distances and, since thermal vibrations are eliminated, can only be associated with correlation between atoms within grain boundaries or dislocations. The effect of thermal vibrations, in the case of the high-temperature system, overwhelms the microstructural features at fine scales ($n = 6$–9).

2.2.2. CWM method. In a first stage we illustrate the concept of the CWM for a hypothetical 1D (energy) map. Let us imagine that this energy map represents a physical system with three characteristic scales, namely a fine, an intermediate and a coarse scale. The insert in figure 6 is a representation of this hypothetical energy map obtained by the linear superposition of three sinusoidal functions with three different periods, namely a small, intermediate and large period. The spatial axis (X) is discretized into 512 points. The wavelet transform of the energy map produces 512 coefficients. The first 256 wavelet coefficients correspond to the decomposition of the energy map at the finest scale $n = 9$. The next 128, 64, 32, 16, 8, 4, 2 and 1 entries are for the scales 8, 7, 6, 5, 4, 3, 2 and 1. The total energy, E, as a function of scale, n, is calculated

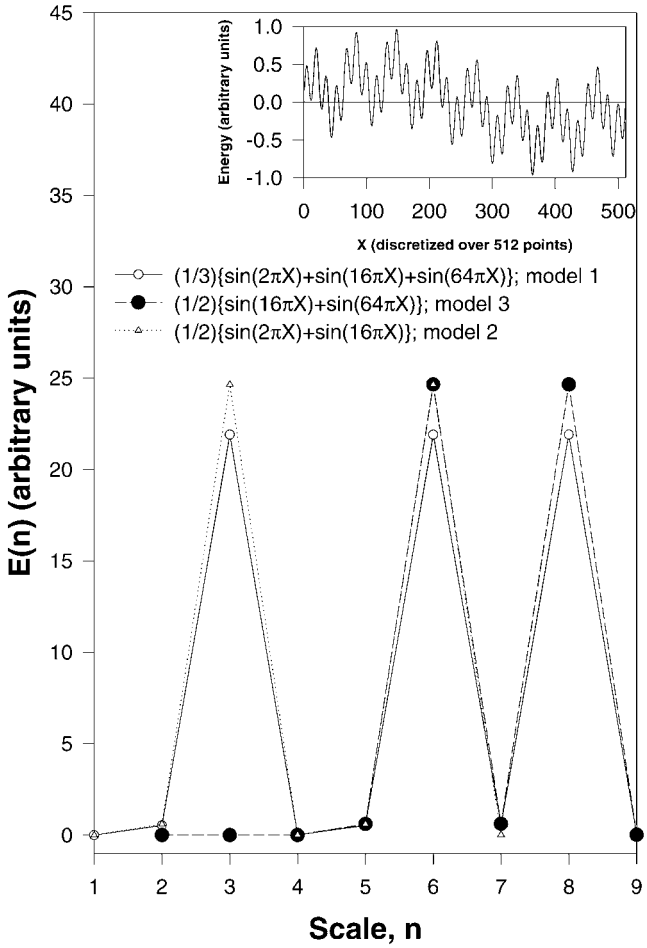

Figure 6. Illustration of the CWM method through hypothetical 1D energy maps. Total energy E as a function of scale is shown for three separate models. The insert shows the map of model one, where the horizontal axis denotes space, X, discretized into 512 points. The vertical axis of the insert is the 'energy' given by the superposition of three sine functions with different periods. Model two contains only the intermediate and large periods and uses a discretized space of 128 points. Model three contains only the intermediate and small periods, defined over a region X half of that of models one and two and uses 256 points.

as in section 2.2.1. The total energy versus scale for that system exhibits three maxima. The maxima at scales $n = 8$, 6 and 3, represent the amount of energy associated with features at the fine, intermediate and coarse scales, respectively. We now may consider an approximate model (model two) that describes that physical system over only the intermediate and coarse scales. An energy map produced by this model (not shown in figure 6) may then be obtained by the superposition of only two sinusoidal functions with the intermediate and large periods. This second model, also, represents the physical system with the same spatial dimensions as the first. Space, however, for this second model is discretized into only 128 points, thus the wavelet transform produces 128 coefficients. Out of the 128 coefficients, 64, 32, 16, ..., 2 and 1 represent the phenomenon at scales $n = 7, 6, 5, \ldots, 2$ and 1. Calculation of E at the different scales allows us to report the total energy as a function of scale for that second model

in figure 6. Its energy shows two peaks at the intermediate scale of six and at the coarse scale of three. This model is unable to represent the physical system at fine scales 8 and 9. A third approximate model is now considered. This models the system over a region of space half the size of the other two. Space is discretized into 256 points. The energy map is the sum of the two sine functions with the fine and intermediate periods. This model produces 256 wavelet coefficients. The finer scale of the third model is equivalent to the finer scale of the first one, so the first group of 128 wavelet coefficients is associated with scale 9, the next group of 64 with scale 8, etc, with the last coefficient corresponding to scale 2. Scale 1 is not defined for this smaller model. The total energy against scale has two maxima at $n = 6$ (intermediate scale) and $n = 8$ (fine scale). We can now use the fact that the approximate models two and three overlap in scale to construct a compounded model statistically equivalent to model one. In other words, model one (reminiscent of a large L-J system) is statistically equivalent to the combined models two and three (reminiscent of a Potts and small L-J models, respectively), as is evidenced from figure 6. Here, the relevant statistical information extracted from each model is simply E. As can be seen in figure 6, the E values for model one are similar to those obtained by combining models two and three. The intermediate scales (around $n = 6$) are common to both models two and three; this overlapping is essential for bridging the two models.

Let us suppose now that the physical system under consideration may evolve in time by exchange of energy between structural features at the three different scales. A study of energy transfer between the fine scale features to coarse features via the overlapping intermediate scale is therefore made possible by considering the time evolution of the compound system in place of that of the first model. If model one is computationally intensive, but not models two and three, it is therefore possible to achieve the same output with lower cost. Here, model three was half the size of the expensive model one. Yet, the CWM can be used with much higher efficiency, for example, by combining a model three, being several times smaller than model one, and a correspondingly sized model two.

Having shown the importance of overlap for bridging models at different scales, we now return to the grain growth problem. Wavelet analysis of a MD energy map provides its wavelet transform coefficients from the atomic to the coarsest scale (corresponding to the physical dimensions of the system). Similarly the wavelet coefficients of a MC map extend over scales ranging from the lattice spacing to the system size. Let us consider a Q-states Potts model and an L-J system that may have different physical dimensions. The range of scales for both systems overlap provided the Potts model is larger than the L-J system and the lattice spacing of the Potts model is not too coarse. The coarser scales of the L-J model may then correspond to the finer scales of the Potts model. A compound matrix of wavelet coefficients is then formed such that at those scales common to the L-J and Potts systems the statistical properties of the coefficients are those of the L-J system; at coarser scales the statistical properties of the coefficients are those of the Potts model. This yields a wavelet compound matrix representing the phenomenon of grain growth over the interval of scales now being the union of the intervals treated individually by the two models.

As an example, we consider an L-J system of 1×1 units of length discretized into 256×256 points. Next we consider a larger Potts system with a physical size of 2×2 units of length discretized into 128×128 points. Figure 7 illustrates the construction of the compound matrix. Consider that in figure 7(a) are the wavelet coefficients of the L-J system and in figure 7(b) are those of the Potts system. Note that the discretization and the units of length can vary, and this is only an example illustrating the ideas. The problem addressed herein is that the Potts system cannot represent the details 'seen' by the L-J system. Submatrix A shown in figure 7(b) represents the details appearing when 2×2 units of length are discretized into 64×64 points; yet this is equivalent to 1×1 units of length discretized into 32×32 points. The same type

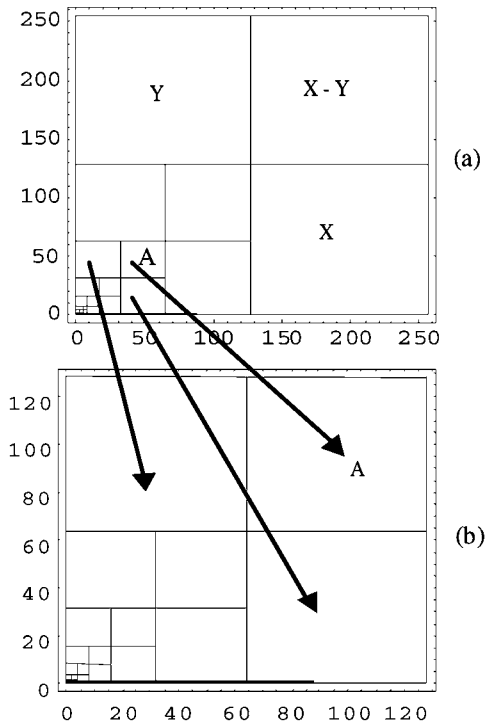

Figure 7. Schematic diagram of the construction of the CWM: (a) from the L-J system of 1×1 units of length discretized into 256×256 points and (b) from the Potts system of 2×2 units of length discretized into 128×128 points. The arrows indicate the substitution (transfer of matrix statistics) of matrices in forming the compound matrix. Only three such substitutions are shown for illustration.

of discretization (1×1 units, 32×32 points) in the L-J system is represented by submatrix A in figure 7(a). Thus, by making the substitutions as indicated by the arrows, the compound matrix has now statistical information at those scales not 'seen' by the Potts model, yet seen by the L-J models. Of course, all the corresponding matrices (those with corresponding scale and discretization) are substituted, yet only three such substitutions are shown in figure 7. The compound matrix is a representation of the microstructure over the range of scales which is now the union of the scales of the L-J and Potts systems.

In order to illustrate the CWM method, we now consider the grain growth process in a small L-J system, one-quarter times smaller than that described before. This smaller atomic system consists of 22 500 particles in a cell with an edge length of about 0.0503 μm. The initial microstructure was prepared exactly in the same way as in the case of the larger L-J system. All other conditions are the same as those used in the case of the large L-J system discussed previously. The time evolution of the potential energy is similar to that of the larger system and after 400 000 time integration steps the potential energy has decreased by approximately 63% of the initial potential energy. Because the small L-J system is only a quarter of the larger one, its energy map is projected on a (256×256) matrix. We show in figure 8 the initial and final energy maps of that system.

We now demonstrate that the compound matrix of wavelet coefficients constructed from this small MD system and the larger MC systems contains similar information, scale-wise, as the large MD system. Figure 9 shows the energy for the three systems with respect to scale.

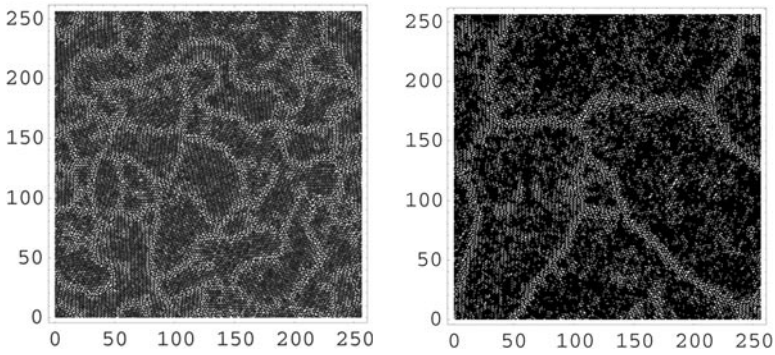

(a) (b)

Figure 8. (a) Initial and (b) final energy maps for the small L-J system. Since this system is one-quarter of the larger L-J system reported in figure 2, the energy is mapped on (256 × 256) matrices.

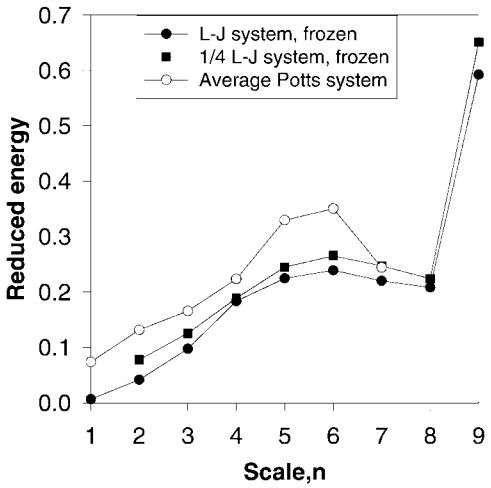

Figure 9. Energy of the wavelet representation of the energy map of the small L-J system annealed and frozen (full squares), the large L-J system annealed and frozen (full circles) and an average annealed Potts system (open circles). The scales are defined as in figures 5 and 6 for the Potts and large L-J systems. The coarsest scale of the small L-J system calculated from 1 × 1 points starts at the value two since the physical dimensions of the small L-J system are two times smaller than those of the Potts system or large L-J system.

At each scale the energy was evaluated in a manner identical to that described in section 2.2.1. We have used energy maps from frozen microstructures in order to minimize the contribution of thermal vibration to the energy of the small and large L-J systems. We have also averaged the four energy against scale plots of the final Potts systems previously reported in figure 4 to produce an average Potts system. For the small MD system (designated as '1/4 L-J' in figure 9), the plot contains eight points (scales 2–9) corresponding to resolutions of 1 × 1 (two on the horizontal axis), ..., 64 × 64 (eight on the horizontal axis) and 128 × 128 (nine on the horizontal axis). Since this system is physically one-quarter of the MC system these scales correspond to the large MD system with resolution of 2 × 2 (scale 2), ..., 128 × 128 (scale 8) and 256 × 256 (scale 9).

All three plots show very similar behaviour in the interval of scales from one to seven: a maximum between five and six representing the grain size, and a monotonic decrease toward the continuum limit. The small L-J and large L-J models agree quite well with each other although the energy of the small system exceeds consistently, but only slightly, that of the larger one. It is unclear at this stage whether this difference is due to a size dependence. The energy of the average Potts system is also slightly larger than the energy of the L-J system. Since this difference is particularly significant near scales 5 and 6, it can be attributed to differences in grain boundary energies. One expects such a difference between a Potts model that has only limited anisotropy in the grain boundary energy (i.e. related to grain boundary inclination) and L-J systems with grain boundaries that may take on a very wide range of energies depending not only on inclination, but also on grain misorientation. Let us stress that these differences are not due to a weakness of the wavelet analysis, but only of the incomplete quantitative correspondence between the Potts and L-J models. A better overlap in the energy representations of the wavelet matrices at different scales could be achieved between the L-J system and the Potts systems provided that the orientation anisotropy is included in the latter. Yet, we have used the simplest Potts and L-J models and leave such issues for future research.

In spite of these small quantitative differences, we next illustrate further how the wavelet transforms obtained from the small L-J system and the Potts model may be combined to construct a wavelet matrix statistically equivalent to that of the large L-J system. The average Potts system and the small L-J system overlap at scales 2–7 and show similar trends in their energy versus scale. However, the Potts model lacks information on small-scale features (scales 8 and 9), which are now provided by the small L-J system. The small L-J system lacks information on large-scale features. Construction of a CWM from the small L-J system and the Potts model leads to a description of the microstructure (over a combined range of scales from one to nine) statistically equivalent to that of the wavelet transform of the large L-J system. Such a CWM produces a plot, energy against scale, superposition of two plots (Potts and small L-J) over all scales from one to nine. Note that the resolutions at scales on the left-hand side of figure 8 are quite small and thus a large number of simulations would be, in general, required to obtain useful information. However, the bridging of the simulation is most important at higher resolution scales, for example seven to nine.

In this example, we considered systems smaller than those current computers are able to handle. Yet, it illustrates that we can run (at low computational cost) an MD simulation containing only 22 500 atoms and the computationally cheap MC calculation to obtain a wavelet transform matrix with statistical properties similar to those of the much more time-demanding MD simulation of 90 000 atoms. Obviously, as the two systems (Potts and small L-J) get further apart in scale, the error in the representation of the energy increases. Importantly, since it is relatively inexpensive to solve large Potts systems it is feasible for the two systems to have a number of overlapping scales.

3. Conclusions

We have illustrated how the mathematical tool of wavelet transformation can be used to analyse the microstructure of 2D polycrystalline systems as well as their evolution during normal grain growth. The wavelet analysis presented here enables the shedding of light on how structural features with different spatial scales contribute to the energy of a microstructure. We provided an illustrative example demonstrating the great potential of using wavelet analysis to bridge computer simulation techniques that model the phenomenon of grain growth over different ranges of scale. In order for the bridging of the two methods to be efficient, a number of overlapping scales should be assigned; the present study is amenable to establishing the

minimum number of overlapping scales that will not compromise the effectiveness of the CWM method. Furthermore, even though rather straightforward, the effect of improved versions of the models and simulation methods examined remains to be investigated. This, also, provides a 'forum' for comparing various models and simulation techniques. Natural extensions of the process illustrated here include the incorporation of time scaling, with time as an additional axis (the time axis requires, for wavelet analysis, frozen images at certain time intervals), which provides the wavelet coefficients of the atomistic system at coarser spatial and time scales. Furthermore, although this work examined the bridging of only two simulation methods, we can envision bridging the MC/Potts model to some third technique for simulation over a larger interval of scales, for example through finite element techniques. This could be accomplished by bridging the wavelet transform data of MC simulations to those produced from finite elements.

Acknowledgment

Support from NSF grant CMS-9812834 is acknowledged.

References

[1] Olson G B 1997 *Science* **277** 1237
[2] Kurtz S K and Carpay F M A 1980 *J. Appl. Phys.* **51** 5725
[3] Atkinson H V 1988 *Acta Metall.* **36** 469
[4] Hillert M 1965 *Acta Metall.* **13** 227
[5] Hunderi O and Ryum N 1996 *Acta Mater.* **44** 1673
[6] Mulheran P A 1992 *Phil. Mag. Lett.* **65** 141
[7] Mulheran P A 1994 *Acta Metall. Mater.* **42** 3589
[8] Fradkov V E and Udler D 1994 *Adv. Phys.* **43** 739
[9] Pande C S 1987 *Acta Metall.* **35** 2671
[10] Pande C S 1993 *Modelling of Coarsening and Grain Growth* ed C S Pande and S P Marsch (Chicago: The Minerals, Metals and Materials Society)
[11] Pande C S and Dantsker E 1994 *Acta Metall. Mater.* **42** 2899
[12] Deymier P A, Vasseur J O and Dobrzynski L 1997 *Phys. Rev.* B **55** 1
[13] Nichols C S, Cook R F, Clarke D R and Smith D A 1991 *Acta Metall. Mater.* **39** 1657
[14] Romero D, Martinez L and Fionova L 1996 *Acta Mater.* **44** 391
[15] Shvindlerman L S, Sursaeva V G, Yashnikov V P and Faulkner R G 1994 *Interface Sci.* **2** 153
[16] Mason T A and Adams B J 1994 *J. Metall.* **46** 43
[17] Sahni P S, Grest G S, Anderson M P and Srolovitz D J 1983 *Phys. Rev. Lett.* **50** 263
[18] Chen L Q 1995 *Scr. Metall. Mater.* **32** 115
[19] Soares A, Ferro A C and Fortes M A 1985 *Scr. Metall.* **19** 1491
[20] Tadmor E B, Phillips R and Ortiz M 1996 *ACS J. Surf. Colloids (Langmuir)* **12** 4529
[21] Mullins M and Dokainish M A 1982 *Phil. Mag.* A **46** 771
[22] Kitagawa H, Nakatami A and Sibutani Y 1994 *Mater. Sci. Eng.* A **176** 263
[23] Heermann D W 1986 *Computer Simulations Methods in Theoretical Physics* (Berlin: Springer)
[24] Holm E A, Glazier J A, Srolovitz D J and Grest G S 1991 *Phys. Rev.* A **43** 2662
[25] Anderson M P, Srolovitz D J, Grest G S and Sahni P S 1984 *Acta Metall.* **32** 783
[26] Ling S, Anderson M P and Grest G S 1992 *Mater. Sci. Forum* **94–96** 39
[27] Gao J and Thompson R G 1996 *Acta Mater.* **44** 4565
[28] Daubechies I 1992 *Ten Lectures on Wavelets* (Philadelphia, PA: SIAM)